Computer Simulations on the Free Energies and Phase Diagrams of Asymmetrically Interacting Blends

Sanat K. Kumar

Department of Materials Science and Engineering, The Pennsylvania State University, University Park, Pennsylvania 16802

Received September 10, 1996; Revised Manuscript Received May 5, 1997[⊗]

ABSTRACT: We consider binary polymer blends where the energetic interactions between the three different pairs of monomers are not equal to each other. From computer simulations in the isothermal−isobaric ensemble, we show that these disparate energetic interactions yield different packing behavior even at the level of the pure components. This results in the pure materials having unequal densities and cohesive energies. In the context of mixtures we have considered two cases. In the system termed "attractive" we have employed Lennard−Jones interactions which favor the formation of dissimilar 1−2 contacts. The residual chemical potential changes on mixing for both components, independently, appear to vary parabolically with system composition. If one chose to model these results with the Flory model [or alternately, the polymer analog of the regular solution theory], then the chemical potential changes on mixing for each component would appear to be describable by a composition independent value of the χ parameter. However, the effective χ values derived from the two components are not equivalent. Since this finding violates thermodynamic consistency, it implies that the effective single χ parameter characterizing the free energy of mixing must be composition dependent. Similar results were obtained in the case of a "nominally athermal" blend, where the 1−2 interaction energy was selected to yield $\chi = 0$ if the blend followed the Flory assumptions of incompressibility and randomly mixed chain segments. We show that these results can be explained on the basis of energetic effects and nonrandom mixing which is triggered by differences in the packing behavior of the pure components. Finally, this packing disparity also causes polymer blends with nominal $\chi = 0$ in terms of the Flory lattice definition to phase separate. This phenomenon is a consequence of the coupling between packing and energetic interactions which yields an unfavorable enthalpy change on mixing. We conclude by emphasizing, in agreement with past theoretical calculations, the importance of packing effects in describing the thermodynamics of polymer systems, an issue which must be included if an improved description of polymer thermodynamics is to be achieved.

1. Introduction

The miscibility of polymer blends is a topic that has been extensively studied[1−11] from both a theoretical perspective and an experimental perspective. Several aspects, such as the effects of compressibility on blend thermodynamics and the role of stiffness and monomer structure disparity on miscibility have been focused on, and each of these factors has been postulated to contribute to the Gibbs energy of mixing.[10,11]

The use of computer simulations for studying the thermodynamics of polymer blends was first proposed by Binder and co-workers.[5,6] In a series of elegant articles these workers have shown that Flory theory is not adequate even to represent the nearly ideal case of symmetric lattice polymer blends where the two pure components are identical in terms of monomer size, monomer structure, bond length, chain length, and energetic interactions. The strength of interactions between dissimilar monomers represents the only asymmetry in these systems. Additionally, they suggested that the departures of symmetric blend behavior from Flory theory are consistent with the unusual composition dependences observed for small angle neutron scattering [SANS] determined χ parameters, χ_{SANS}, even in the simplest case of isotopic polymer mixtures.[12,13] In this context we note that the study of the composition dependence of χ_{SANS} is a very popular area of research, as has been reviewed recently in ref 14.

It must be emphasized that one of the major assumptions in the simulations of Binder[5,6] is that the density of the polymer systems are independent of system identity. Kumar[14] has performed computer simulations on symmetric polymer blends, similar in spirit to the model utilized by Binder,[5,6] but with two differences. First, we modeled the systems in free space, in contrast to dealing with lattices. Second, in addition to considering the blends and the homopolymers to be at the same density {i.e., the so called "incompressible" state}, we have also performed simulations where all of the systems were at the same pressure. Consequently, the system density varied with composition. We then evaluated the chemical potential changes on mixing for the two blend components through the chain increment method.[15−18] In agreement with the conclusions of Binder and co-workers,[5] the chemical potential changes on mixing under the "incompressibility" approximation could only be described with a composition-dependent χ. In contrast to these findings, the results under constant pressure conditions could be modeled by the Flory−Huggins form (or more generally by the polymer analog of the regular solution expression for activity coefficients) with a composition-independent χ parameter. While these results stress the importance of the finite compressibility of polymer liquids in determining their thermodynamics, the more surprising result is that these simple blends appear to follow the Flory model when examined under experimentally relevant state conditions.

Since most polymer mixtures will be asymmetric in some aspect, we expect that these past works will not be representative of realistic systems. Here we build on previous work[19−21] and consider blends comprised of polymers of equal length which are energetically asymmetric. The Lennard−Jones parameters defining 1−1

[⊗] Abstract published in *Advance ACS Abstracts,* July 1, 1997.

S0024-9297(96)01348-4 CCC: $14.00

monomer and 2−2 monomer interactions are selected so that: $\epsilon_{22}/\epsilon_{11} = 0.8$. In one set of simulations the 1−2 interaction energy is defined as $\epsilon_{12} = 1.2(\epsilon_{11}\epsilon_{22})^{1/2}$. For this "attractive" blend we find that the residual chemical potential changes on mixing for each component follow a parabolic dependence on composition, suggesting that they could be described by composition-independent values of the Flory parameter, χ. However, the effective χ values derived from the chemical potentials of the two different components are different. While energetic effects can explain some of this asymmetry, we show that some other effect, possibly entropic in origin, has to be evoked to obtain a quantitative understanding of these results. To understand this additional effect we consider a situation where the Lennard−Jones cross interaction energy is $\epsilon_{12} = (\epsilon_{11} + \epsilon_{22})/2$. This particular value of ϵ_{12} is selected since the nominal interaction parameter, defined as $\chi \propto [2\epsilon_{12} - (\epsilon_{11} + \epsilon_{22})]$, is exactly equal to zero if the blend followed the Flory assumptions of randomly mixed chains on an incompressible lattice.[22] Consequently, energetic effects are minimized in this case. In agreement with the results on the attractive system, we find that the chemical potential changes on mixing for the components of this "nominally athermal" blend as a function of composition are not symmetric. On general grounds we show that these differences in behavior for the two species in both the attractive and the nominally athermal blends arise directly from nonrandom mixing [or packing asymmetries]. Since many cruder models for polymer thermodynamics assume that chain segments mix randomly, we suggest that these theories cannot successfully capture the essence of these findings.

Finally, we had expected, based on the past predictions of Sanchez,[3] that the nominally athermal system should be miscible under most conditions since the enthalpic contribution to χ is 0 if the system were randomly mixed and incompressible. These systems, however, could show lower critical solution [LCST] behavior at high temperatures due to the mismatch in equation-of-state properties of the two pure components. In contrast to these expectations, we find, through the use of the semigrand ensemble method,[5,23] that blends comprised of chains of length $N = 100$ phase separate with a well-defined upper critical solution temperature [UCST]. We show that the miscibility of these blends can be predicted reasonably well by Flory−Huggins (or regular solution) theory if the χ parameter is estimated not by its bare Flory definition but from the following relationship:

$$\chi = \frac{V_m}{RT}(\delta_1 - \delta_2)^2 \tag{1}$$

Here V_m is the molar volume of the liquid and δ_i is the Hildebrand solubility parameter of pure component i.[24] Note that since the solubility parameter incorporates the effects of packing in determining the enthalpy changes on mixing, the coupling between energetics and packing [or entropy] plays a critical role in determining the miscibility of these polymeric systems.

The rest of the paper is organized as follows. Section 2 describes the Monte Carlo method employed in this work and the models considered. Special emphasis is placed on delineating the method utilized to enumerate the chemical potential changes on mixing. Section 3.1 discusses results on the two pure polymers considered in this work, while section 3.2 summarizes our findings on the attractive blends. Section 3.3 then extends these ideas to the nominally athermal blends, while section 3.4 presents a brief discussion of these results. Section 4 describes the phase diagrams obtained using the semigrand ensemble method for these systems. Finally, section 5 summarizes our major findings.

2. Model and Simulation Procedure

2.1. Model. Polymer chains were modeled as beads of diameter σ, connected by harmonic springs as in our past work.[14−16] The beads of both blend components were of identical diameter, and both chains were of identical length, or degrees of polymerization, N. Two different situations corresponding to $N = 25$ and 100, respectively, were considered. Nonbonded polymer beads of type i and type j, respectively, were assumed to interact through a standard Lennard−Jones potential

$$u(r_{ij}) = -4\epsilon_{ij}\left[\left(\frac{\sigma}{r_{ij}}\right)^{12} - \left(\frac{\sigma}{r_{ij}}\right)^{6}\right]; \qquad r_{ij} < r_c \tag{2}$$

where r_c is a cutoff distance beyond which the potential is set to zero. We normally set r_c to 2.5σ, although we have employed a value of 4σ in the extremes of composition for the $N = 25$ system. Long-range corrections for thermodynamic properties were included by assuming that the radial distribution functions attained a value of unity for distances beyond r_c.[25] For example, the reduced long-range correction for the internal energy, U^*_{lr}, of a pure polymer melt is,

$$U^*_{lr} \equiv \frac{U_{lr}}{\epsilon} = \frac{2\pi\rho^*}{\sigma^3}\int_{r_c}^{\infty} r_{ij}^2 \frac{u(r_{ij})}{\epsilon} dr_{ij} \tag{3}$$

where $u(r_{ij})$ is the Lennard−Jones potential, $\rho^* = \rho\sigma^3$ is the reduced monomer density, and ϵ is the well depth of the potential. This integral can be evaluated analytically. For the cases tested for $N = 25$, we found no systematic differences in properties with the two different cutoff lengths. Also, we have employed $r_c = 2.5\sigma$ in all of our simulations for $N = 100$. For $N = 25$ we have utilized simulation cells with 32 chains, although systems with 100 chains were utilized in the extremes of composition, i.e., for $\phi \le 0.06$ or $\phi \ge 0.94$. For $N = 100$ the systems consisted of 25 chains. The pure component energetic parameters were not equal to each other and we employed the following definitions:

$$T^* \equiv \frac{k_B T}{\epsilon_{11}} \tag{4}$$

$$\frac{\epsilon_{22}}{\epsilon_{11}} = 0.8 \tag{5}$$

A majority of our calculations were conducted for a temperature $T^* = 2$. The only quantity that remains to be defined is the cross interaction energy parameter, ϵ_{12}, and we have considered two different cases. In the case termed **attractive**

$$\epsilon_{12} \equiv 1.2\sqrt{\epsilon_{11}\epsilon_{22}} \tag{6}$$

i.e., $\epsilon_{12}/\epsilon_{11} \approx 1.08$. We have also defined the **nominally athermal blend** as

$$\epsilon_{12} \equiv \frac{\epsilon_{11} + \epsilon_{22}}{2} \tag{7}$$

i.e., $\epsilon_{12}/\epsilon_{11} = 0.9$. If the blends followed the Flory

assumptions of incompressibility and random mixing, then the interchange energy parameter, χ, defined as

$$\chi = -\frac{z}{k_B T}\left[\epsilon_{12} - \frac{\epsilon_{11} + \epsilon_{22}}{2}\right] \tag{8}$$

would be negative for the attractive blend, while it would be identically equal to zero for the nominally athermal mixture. Here z is the lattice coordination number

The simulations were conducted following the Metropolis Monte Carlo algorithm as has been reported in past work.[14,15] The exploration of phase space was achieved by reptation and crank shaft moves. In addition, we have also employed a swap move where the position of a molecule of type 1 and one of type 2 were exchanged as part of an elementary move. This move helps in the rapid equilibration of systems which are dilute in one component, and is also accepted following the Metropolis criterion. To mimic experimentally realistic conditions, we have simulated the systems in the isothermal−isobaric ensemble by permitting volume fluctuations. To model systems at atmospheric pressure we set the reduced pressure as follows:

$$P^* = \frac{P\sigma^3}{\epsilon_{11}} = 0 \tag{9}$$

This follows, since, for typical polymer melts, the $\sigma \approx 5$ Å, while $\epsilon_{11}/k_B \approx 100$ K. For a pressure of 1 bar, this yields $P^* = 0.005$. Given the uncertainties in properties encountered in typical simulations, this number is virtually identical to 0. Each simulation involved in excess of 100 million attempted elementary moves (i.e., reptation, crank shaft, or particle swap moves). Volume changes were attempted every 2000 attempted elementary chain moves. Various quantities calculated in the simulations included the total system volume, pressure, and energy. In addition, the incremental chemical potentials of both components were also enumerated as will be described below.

2.2. Calculation of Chemical Potentials. The primary quantities obtained from the simulations were the incremental chemical potentials[15] of both components, $\mu_r^i(N+1)$. As noted in previous work,[14−18] the incremental chemical potential of a chain of type i and length x, $\mu_r^i(x+1)$, in a mixture is defined as

$$\mu_r^i(x+1) = \mu_{chain}^{r,i}(x+1) - \mu_{chain}^{r,i}(x) \tag{10}$$

where $\mu_{chain}^{r,i}(x)$ is the residual chemical potential of a chain of type i and of length x [$\equiv \mu_{chain}^{i}(x) - \mu_{chain}^{ID,i}(x)$, where $\mu_{chain}^{i}(x)$ is the chemical potential of a chain of type i of length x, and $\mu_{chain}^{ID,i}(x)$ is the corresponding ideal gas value]. Since the incremental chemical potential is a function of x, the exact expression for the residual chemical potential of a chain of type i, $\mu_{chain}^{r,i}(N)$, is

$$\mu_{chain}^{r,i}(N) = \sum_{x=1}^{N} \mu_r^i(x) \tag{11}$$

Although $\mu_r^i(x)$ is strictly a function of x, often the incremental chemical potential reaches an asymptotic value at $x > 4$ especially for flexible bead−rod and bead−spring chains such as those considered in this work.[14−18] This allows us to use the relationship which becomes asymptotically correct for long chain length polymers

$$\mu_{chain}^{r,i}(N) \approx N\mu_r^i(N+1) \tag{12}$$

where $\mu_r^i(N+1)$ is the incremental chemical potential for the $(N+1)$th polymer segment. From here we define $\Delta\mu_r$, the residual chemical potential change on mixing, as

$$\beta\Delta\mu_r^i \equiv \beta\mu_r^i(N+1) - \beta\mu_r^{pure,i}(N+1) \equiv \chi_i(1-\phi_i)^2 \tag{13}$$

This quantity has direct significance to our interpretation, which is based primarily on the Flory−Huggins theory. The last equivalence defines the value of the effective χ parameter for component i in the blend. Note that, in our simulations, these quantities are evaluated in the isothermal-isobaric ensemble as in ref 14.

2.3. Enumeration of Polymer Phase Equilibrium. In the case of the nominally athermal system, we shall examine the possibility of liquid−liquid phase separation. Standard methods for the simulation of phase equilibria in small molecular systems, such as the Gibbs ensemble technique,[26] are difficult to apply to polymeric systems since an important elementary move in these simulations is the random insertion of a chain into a frozen snapshot of the system of interest. Due to the length of the molecules (typically $N \geq 25$) this represents a move with an extremely small probability of acceptance. While recent developments[27] involving the partial insertion of chains appear to offer promise in alleviating these problems, we have employed a somewhat different technique, termed the "semigrand ensemble" method,[23] to simulate phase equilibria in polymer systems. Here we shall summarize the method.

Simulations are conducted in a standard isothermal−isobaric ensemble. To locate phase coexistence we attempt random identity changes as an elementary move in our simulations. Note that this move serves to alter the overall composition of type 1 and type 2 molecules in the simulation cell and is therefore different from the particle swap elementary move discussed above, which always conserves the number of type 1 and type 2 chains in the system. The acceptance criterion for these identity changes is then controlled by the set value of the exchange chemical potential, $\Delta\mu \equiv \mu_{chain}^{2}(N) - \mu_{chain}^{1}(N)$

$$P_{acc} = \exp(-\beta\Delta U)\exp(\beta\Delta\mu) \tag{14}$$

where the identity of a randomly chosen molecule, which is of type 1 in this particular example, has been exchanged for a molecule of type 2. Further details of this sampling procedure are illustrated in ref 23: the method we employ is termed as type a in this reference. The technique then involves performing a series of simulations, each with a different set value of $\Delta\mu$. The average composition in the simulation cell is monitored in each case. Phase coexistence envelopes are identified by a discontinuous change in composition and system density with slight changes in the value of $\Delta\mu$.

While this method gives a measure of the compositions in coexistence, the occurrence of a first-order phase transition is frequently accompanied by significant hysteresis. Consequently, the compositions derived from these simulations need not be accurate measures of phase coexistence, but are reflective of some composi-

Table 1. Thermodynamic Properties Obtained for Pure Components at $T^* = 2$ and $P^* = 0$[a]

material	chain length N	density $\rho^* \equiv \rho\sigma^3$	liquid energy U^*_{liq}	gas energy U^*_{gas} ($\rho^* = 0$)	δ^*	$\beta\mu_r$ ($N + 1$) (liquid)
1	25	0.688_1	-2.771_2			1.27_2
2	25	0.584_1	-1.462_2			1.62_2
1	100	0.698_1	-2.784_4	-0.560	1.246	1.24_6
2	100	0.598_1	-1.477_2	0.107	0.973	1.63_7

[a] The numbers reported as subscripts are error bar estimates. Hence 0.688_1 implies 0.688 ± 0.001.

tion intermediate between the binodal and spinodal values. In previous work Kofke and Glandt[23] had suggested that accurate values of the binodal compositions could be determined by calculating the chemical potentials of the different components in the system and finding that point in phase space where the chemical potentials of all components are identical across the phases in equilibrium. We have attempted to follow this procedure but find that the typical errors in $\beta\mu_r$ are $\approx$ 0.02. Hence, for a chain length $N = 100$, the uncertainties in the chemical potentials are $\approx 0.02 \times 100 = 2.0$. Since the residual chemical potentials of each component change by roughly this magnitude over the whole range of composition, it becomes virtually impossible to properly identify the point where the chemical potential equality criterion is satisfied. Consequently, we report values for phase coexistence obtained from the semigrand ensemble simulations, with the understanding that these quantities will typically be associated with relatively large error bars.

3. Results and Discussion

3.1. Pure Components. We begin by considering the behavior of the two pure polymers which were simulated in this work. In the case we shall discuss here $T^* = 2$ and $P^* = 0$ for both $N = 25$ and 100. We find that the more strongly attractive component (component 1) has a higher liquid density under these conditions (see Table 1). Further, the liquid density for both components increase with increasing chain length. The energy of the liquid phase becomes more cohesive for longer chains, a result which can be rationalized with the trends observed for the condensed phase density. These results are consistent with intuitive expectations. The stronger bare attractions in the case of component 1 also manifest themselves as a better packing of chains, as shown in Figure 1, where the *intermolecular* pair distribution function, $g_{inter}(r)$, is plotted as a function of r for chains of length $N = 100$. The intermolecular pair distribution function is defined exactly as a normal $g(r)$ except that all intramolecular contacts are ignored in the counting. Note that Flory theory would not have anticipated these results since it assumes that the segments of the chains are randomly distributed about each other [i.e., $g(r) = 1$ for both intramolecular and intermolecular contacts]. Similar conclusions may be expected for any theory that assumes that chain segments are randomly mixed. A direct consequence of this stronger packing is that component 1 has a larger solubility parameter, δ,[24] than component 2. The dimensionless solubility parameter, δ^*, is defined as

$$\delta^* = \frac{\delta\sigma^{3/2}}{\epsilon^{1/2}} \equiv \sqrt{(U^*_{liq} - U^*_{gas})/V^*_{liq}} \qquad (15)$$

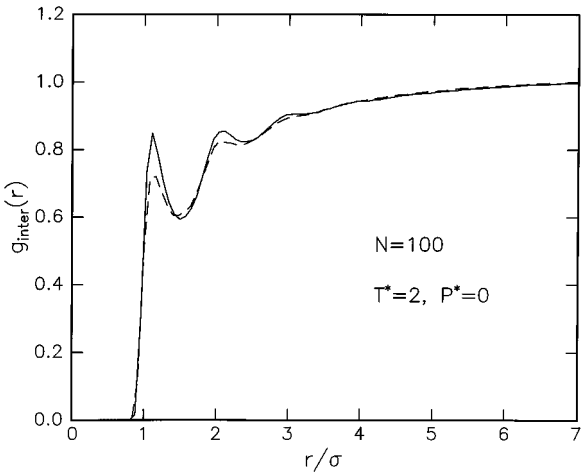

Figure 1. Intermolecular pair distribution functions, $g_{inter}(r)$, as a function of r for the two different pure components of length $N = 100$ at $T^* = 2$ and $P^* = 0$. Key: (—) is for component 1, (– –) is for component 2.

where each internal energy, U^*, is evaluated through the relationship

$$U^* = 2\pi\rho^* \int_0^\infty \left(\frac{r}{\sigma}\right)^2 g_{total}\left(\frac{r}{\sigma}\right) \frac{u(r)}{\epsilon} \, d\left(\frac{r}{\sigma}\right) \qquad (16)$$

$g_{total}(r)$ is the total pair distribution function, including both intermolecular and intramolecular contacts. The two relevant states in eq 15 are the saturated liquid state and the equilibrium gas state which we approximate by an isolated chain. $u(r)$ is the pair potential, and ϵ is the Lennard–Jones energy parameter. It is commonly assumed that if the chain conformations do not change in going from gas to liquid, the difference in internal energy between these two states can be described in terms of the intermolecular radial distribution function, $g_{inter}(r)$, alone

$$\delta^2 = 2\pi\epsilon\rho^2 \int_0^\infty \frac{u(r)}{\epsilon} g_{inter}(r) \, r^2 \, dr \qquad (17)$$

Since chain dimensions do change in going from a gas to a liquid state eq 17 is only an approximate relationship. Qualitatively, eq 17 however immediately shows that materials which pack better should have higher solubility parameters (or cohesive energy densities). This conclusion is consistent with our exact numerical findings illustrated in Table 1.

In the framework of van der Waals theory the solubility parameters must scale linearly with liquid density,[28] i.e.

$$\delta = \sqrt{a}\rho \qquad (18)$$

Here a, the van der Waals attractive parameter, is related to the well depth of the Lennard–Jones potential, i.e.

$$a \sim \frac{\epsilon}{\sigma^3}$$

From here it follows that

$$\frac{\delta_2}{\delta_1} \equiv \frac{\rho_2}{\rho_1}\sqrt{\frac{\epsilon_{22}}{\epsilon_{11}}} \qquad (19)$$

In comparison, from the definition of the solubility parameter following eq 17, we obtain the relationship

$$\frac{\delta_2}{\delta_1} \equiv \frac{\rho_2}{\rho_1}\sqrt{\frac{\epsilon_{22}}{\epsilon_{11}}\frac{I_{22}}{I_{11}}} \tag{20}$$

where

$$I_{jj} = \frac{2\pi}{\sigma^3}\int \frac{u_{jj}(r)}{\epsilon_{jj}}\, g_{\text{inter},jj}(r) r^2\, \mathrm{d}r \tag{21}$$

The dimensionless integrals, I_{jj}, reflect the effects of packing behavior coupled to energetics.[2,4] Clearly, van der Waals theory assumes that the ratio of these integrals is equal to unity, thus effectively ignoring any packing disparity between the two components. This assumption is, of course, inconsistent with simulation findings sketched in Figure 1 where the packing is different for the two pure materials in question. Table 1 shows that the densities of the two components for $N = 100$ have a ratio of 0.86, and $(\epsilon_{22}/\epsilon_{11})^{1/2} = 0.9$. Consequently, eq 19, which is the product of these two quantities predicts that the ratio of solubility parameters is 0.77. Further, since $(I_{22}/I_{11})^{1/2} = 0.96$, eq 20 predicts that the ratio of solubility parameters is 0.74. Since both of these numbers are very close to the simulation derived value of 0.76, we conclude that the primary difference between the two pure materials is captured by van der Waals theory. However, as we shall show below, the van der Waals approximation that $I_{22} = I_{11}$ makes qualitative errors in determining the miscibility of blends, especially in the nominally athermal case (see Section 4.2 below). Note also that eq 20 does not predict the ratio of δ's exactly, and this disagreement reflects the failure of the assumption that chain dimensions do not change in going from the liquid to the gas state.

3.2. Attractive Systems. We focus our attention on the attractive systems where the interaction energy between dissimilar monomers are more favorable than interactions between either pair of similar monomers. Results from both the $N = 25$ and the $N = 100$ blends show similar behavior and are therefore discussed in the same framework.

We begin by considering the internal energy of the system, $U^* \equiv U/\epsilon_{11}$, and the monomer density of the blend, $\rho^* \equiv \rho\sigma^3$, as a function of ϕ_1. As can be seen in Figures 2 and 3 there is a strongly favorable excess energy and volume on mixing for these systems, which is consistent with the empirical notion that these blends are strongly miscible. We also plot the excess volume on mixing, defined as

$$\Delta V = \frac{1}{\rho^*} - \left(\frac{\phi_1}{\rho^*_{1,\text{pure}}} + \frac{1-\phi_1}{\rho^*_{2,\text{pure}}}\right) \tag{22}$$

for both chain lengths as an inset to Figure 3. As can be seen, the excess volume changes on mixing become slightly smaller with increasing chain length, although this trend is almost at the limit of uncertainties inherent in our simulation data.

We now examine the residual chemical potential changes on mixing for the two blend components, $\beta\Delta\mu_r^i$, as a function of the mole fraction of component 1, ϕ_1, in Figure 4. We find, apparently independent of chain length, that both chemical potential changes on mixing are favorable verifying that this blend system is miscible at $T^* = 2$. Further, it appears that $\beta\Delta\mu_r^i$ for each component is effectively parabolic in system composition. At first sight, each of the chemical potentials therefore appear to follow the incompressible Flory model and can be described by a composition independent value of the interaction parameter, χ, to within simulation uncertainties (see eq 13). However, the χ values derived for component 2 are definitely more negative than those for component 1, especially if one considers the extremes of composition. Clearly, the incompressible Flory–Huggins description, which utilizes a single composition independent interchange energy parameter, χ, is not adequate to describe system thermodynamics. This conclusion is not surprising since we are dealing with a compressible system. In this case, if one utilized a lattice description, three separate energetic scales are necessary to define system thermodynamics (see for example ref 4). The fact that the free energy of mixing can be described by two separate interaction parameters represents a simple subset of this idea.

To understand this asymmetry in the "χ" values of the two components of the attractive mixture, we must examine if energetic or entropic factors need to evoked. We shall first consider energetic effects. Examination of Figure 3 shows that the density of pure component 1 is about 10% larger than for pure component 2. Con-

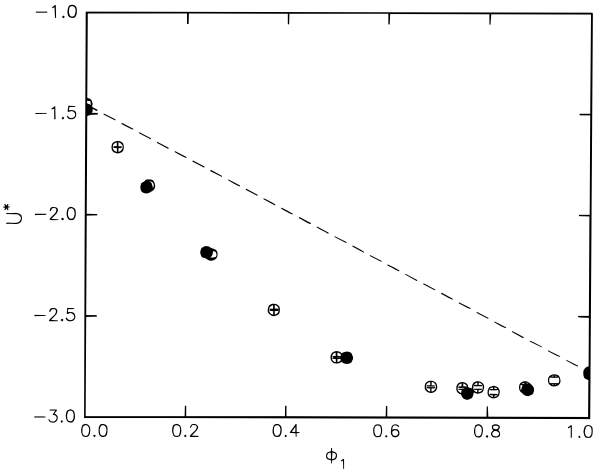

Figure 2. Internal energy, U^*, as a function of mole fraction of component 1, ϕ_1, in the attractive blend at $T^* = 2$ and $P^* = 0$. Key: (○) are for $N = 25$, while (●) are for $N = 100$. The line represents a hypothetical blend with no excess energy change on mixing.

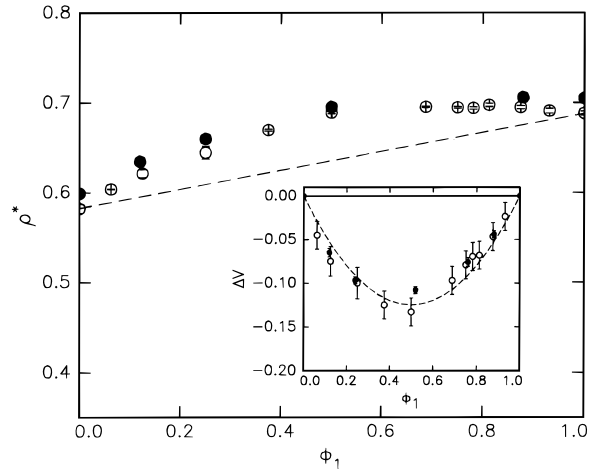

Figure 3. Monomer density, ρ^*, as a function of mole fraction of component 1, ϕ_1, in the attractive blend at $T^* = 2$ and $P^* = 0$. Key: (○) are for $N = 25$; (●) are for $N = 100$. The line represents a hypothetical blend with no excess volume change on mixing. Inset is a plot of excess volume on mixing, ΔV, as a function of ϕ_1. Symbols have the same meaning.

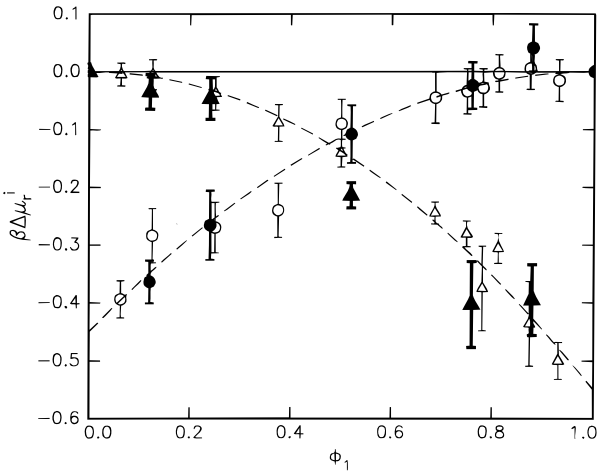

Figure 4. Plot of $\beta\Delta\mu_r^i$ as a function of ϕ_1 for the attractive blend at $T^* = 2$ and $P^* = 0$. For $N = 25$: (○) is for component 1; (△) component 2. The filled symbols correspond to $N = 100$. The lines represent the predictions of Flory theory, eq 13.

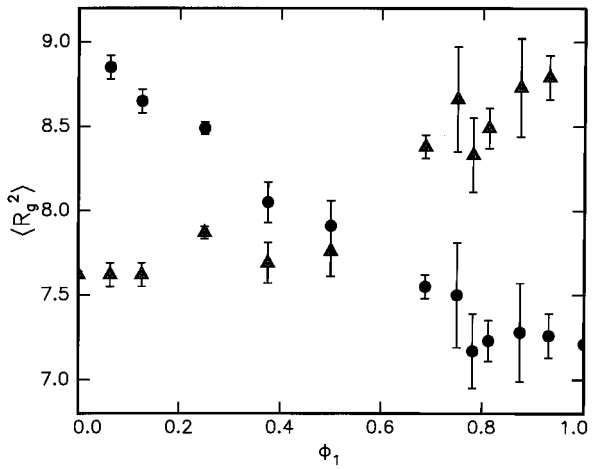

Figure 5. Plot of the mean-squared radius of gyration for attractive blends comprised of $N = 25$ chains plotted as a function of ϕ_1 at $T^* = 2$ and $P^* = 0$. (●) component 1; (▲) component 2.

sequently, since component 1 is more cohesive, it is possible that this factor is sufficient to explain the asymmetry observed in Figure 4. To examine this possibility we consider the internal energy change on mixing, which is equal to the enthalpy change on mixing at $P^* = 0$

$$\Delta U^* = U^* - \phi_1 U_1^* - (1-\phi_1)U_2^* = \phi_1(\bar{U}_1^* - U_1^*) + [1-\phi_1](\bar{U}_2^* - \bar{U}_2^*) \quad (23)$$

where $\bar{U}_i^*$ is the partial molar energy of component i, while U_i^* is the internal energy of pure component i. We shall now define a χ_{energy} parameter and use ϕ in place of ϕ_1

$$\chi_{energy} \equiv \frac{\Delta U^*}{\phi(1-\phi)T^*} \equiv \frac{(\bar{U}_1^* - U_1^*)}{T^*(1-\phi)} + \frac{(\bar{U}_2^* - U_2^*)}{T^*(\phi)} \quad (24)$$

Note that, in general, the χ parameters determined from SANS, chemical potentials, and χ_{energy} are not equal to each other, especially in situations where the χ parameters possess composition dependences. Let us now consider the case where $\phi \to 1$. In this limit we have previously shown that[30]

$$\frac{(\bar{U}_1^* - U_1^*)}{1-\phi} = 0$$

Consequently, we are left with the identity

$$\chi_{energy}(\phi \to 1) = \frac{\bar{U}_2^*(\phi \to 1) - U_2^*}{T^*} \quad (25)$$

The partial molar energies are evaluated from Figure 2 using the relationship

$$\bar{U}_1^* = U^* + (1-\phi)\left[\frac{\partial U^*}{\partial \phi}\right]_{T,P}$$

A similar relationship can be derived for component 2. In the limit $\phi \to 1$ we find $\chi_{energy} = -0.93 \pm 0.02$, while for $\phi \to 0$ we find $\chi_{energy} = -0.82 \pm 0.05$. While the difference in χ_{energy} parameters in the two infinite dilution limits appear to be consistent with the differences in χ values estimated from Figure 4 for the two different components, it is clear that the energetic estimates of χ, i.e., χ_{energy}, are much larger in magnitude than the values observed in the simulations.

As a consequence we are forced to examine additional, entropic origins to explain the trends in Figure 4 on a quantitative basis. It has been proposed in past work that chain dimensions change on blending two polymers.[5,31] To examine this effect in Figure 5 we plot the mean-squared radii of gyration for the two polymers of length $N = 25$ as a function of composition. Clearly, both chains are swollen in all cases, with the maximum swelling being attained when the component is present in infinite dilution. This result, which can serve to reduce the configurational entropy of the chains in question, is a direct consequence of the strong attractive interactions between the two species. We can assess the impact of chain swelling on the chemical potential changes on mixing by examining the entropic loss associated with chain stretching[32]

$$\beta[\mu_r^i(N,\phi_i) - \mu_r^i(N,\phi_i = 1)] \approx \frac{1}{N}\left[\frac{R_{g,i}^2(\phi_i)}{R_{g,i}^2(\phi = 1)} - 1\right] \quad (26)$$

For the two components considered in this work this number is ≈0.02 for $N = 25$ in the limit of infinite dilution where this effect is maximized. Since this effect is much smaller than the discrepancy between the χ's estimated in Figure 4 and χ_{energy} for the two components in their infinite dilute states it appears that chain swelling effects alone cannot reconcile these results. Further credence for this assertion comes from the fact that this entropic argument would predict the effect to be chain length dependent, while our simulation results for chemical potentials appear to be insensitive to chain-length. We can also rule out the ideal gas, translational entropy change associated with the change in system density with composition, since this effect is also on the order of ≈0.01 per segment in the residual chemical potential change on mixing.

The only effect we have not accounted for to this point is the nonrandom packing of the chain segments in the blend. Figure 6 shows results for the three intermolecular pair distribution functions, $g_{inter}(r)$, for $N = 25$ at mirror compositions of ϕ_1 of 0.875 and 0.125, respectively. While 1−2 interactions are preferred over

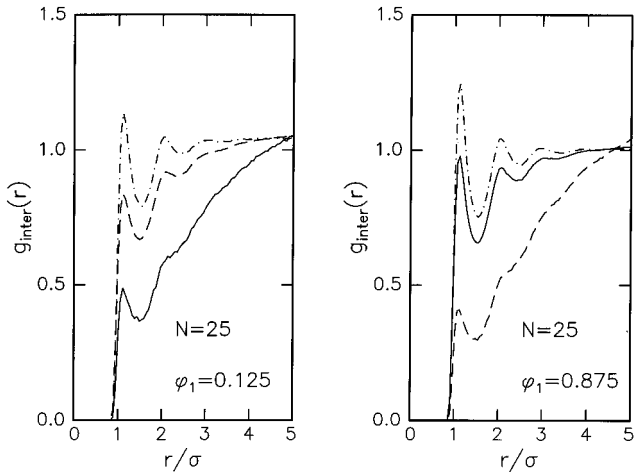

Figure 6. Plot of the three intermolecular radial distribution functions, $g_{ij,\text{inter}}(r)$, as a function of r for attractive blends comprised of chains of length $N = 25$ at two different compositions, ϕ_1, as noted in the figures. Key: (—) 1−1 pairs; (− −) 2−2 pairs; (− · −) 1−2 pairs.

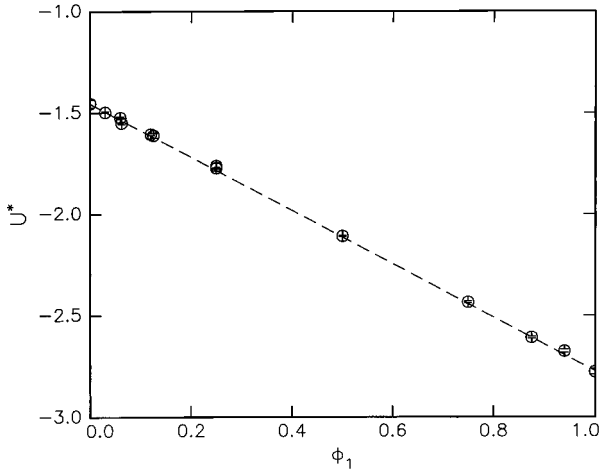

Figure 7. Internal energy, U^*, as a function of mole fraction of component 1, ϕ_1, in the nominally athermal blend at $T^* = 2$ and $P^* = 0$. Key: (○) are for $N = 25$. The line represents a hypothetical blend with no excess energy change on mixing.

intermolecular 1−1 contacts, which in turn are more prevalent than intermolecular 2−2 contacts at $\phi_1 = 0.875$, the probabilities of 1−1 and 2−2 contacts are reversed at $\phi_1 = 0.125$. It is therefore clear that intermolecular 1−1 interactions at $\phi_1 = 0.125$ and the 2−2 interactions at ϕ_1=0.875 are strongly suppressed. This nonrandom mixing effect will contribute an unfavorable contribution to the free energy of mixing and potentially explain the trends observed in Figure 4.[33] While this argument appears plausible and qualitatively explains the trends in Figure 4, it is not conclusive from the evidence presented to this point: consequently, to reiterate this point we shall examine its validity in the context of the nominally athermal systems. This athermal case is particularly useful in this context since we have attempted to set the energetic effects, which dominated the behavior in Figure 4, to zero, and consequently, we should be sensitive to the nonrandom packing effects alone.

3.3. Nominally Athermal System. We begin by considering our results on the nominally athermal blend for $N = 25$. In Figures 7 and 8 we plot the variation of system internal energy, U^* [$\equiv U/\epsilon_{11}$], and monomer density, ρ^*, as a function of the mole faction of component 1 segments in the simulation cell, ϕ_1. These figures

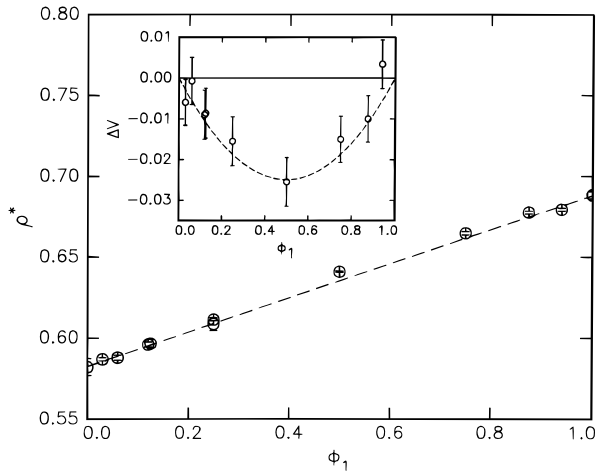

Figure 8. Monomer density, ρ^*, as a function of mole fraction of component 1, ϕ_1, in the nominally athermal blend at $T^* = 2$ and $P^* = 0$. (○) $N = 25$. The line represents a hypothetical blend with no excess volume change on mixing. Inset: plot of excess volume on mixing, ΔV, as a function of ϕ_1. The symbols have the same meaning.

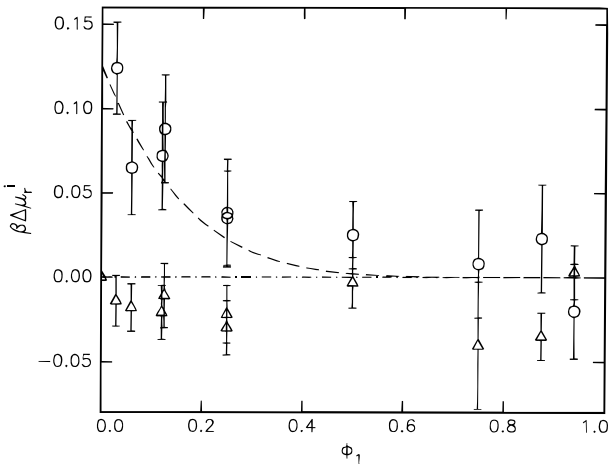

Figure 9. Plot of $\beta\Delta\mu_r^i$ as a function of ϕ_1 for the nominally athermal blend at $T^* = 2$ and $P^* = 0$. For $N = 25$: (○) component 1; (△) component 2. The lines represent guides to the eye.

suggest that the energetic and volumetric properties of these blends are essentially linear combinations of the properties of the two pure components. Further, the inset to Figure 8, which is a plot of the excess volume on mixing, is clearly negative over much of the composition range. Since negative values of ΔV imply that the molecules of the different species "like" each other, this traditionally has been viewed as a sign of miscibility.

We now consider the chemical potential changes on mixing for the two components as a function of ϕ_1 in Figure 9. The residual chemical potential change on mixing for component 2, the less attractive species, is effectively zero independent of composition. This result is consistent with the notion that this miscible blend should be characterized by a χ value of 0 following eq 8. However, the residual chemical potential changes on mixing for component 1 are clearly positive, implying that this component is "destabilized" on blending. Note, however, that this short chain blend is still miscible in these cases. This asymmetry in behavior for the chemical potential changes on mixing for the two blend components is consistent with the results observed for the attractive blends.

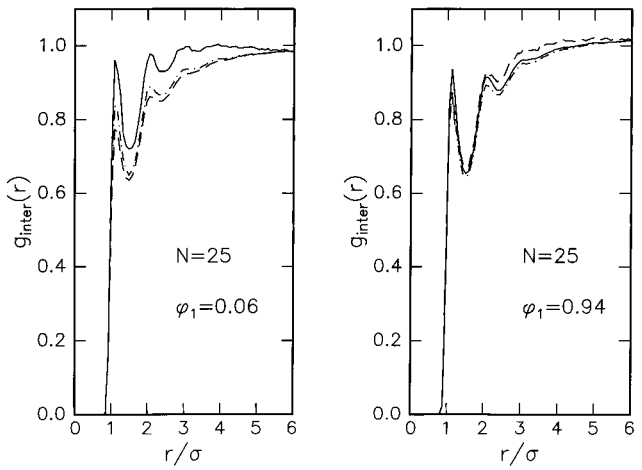

Figure 10. Plot of the three intermolecular radial distribution functions, $g_{ij,\text{inter}}(r)$, as a function of r for the nominally athermal blends comprised of chains of length $N = 25$ at two different compositions, ϕ_1, as noted in the figures. Key: (—) 1−1 pairs; (– –) 2−2 pairs; (– · –) 1−2 pairs.

To understand these conclusions, we first note that excess energy gain on mixing is effectively zero for both components. Thus, an energetic argument would suggest that $\chi_{\text{energy}} \approx 0$, independent of composition. In contrast to the energetic blend, the results observed in Figure 9 cannot be explained even partly by energetic effects. Similarly, R_g values for both components are essentially unaffected by blending. Consequently, in Figure 10 we consider the three intermolecular radial distribution functions for two extremes in composition, $\phi_1 = 0.94$ and 0.06, respectively, to examine if nonrandom mixing can explain the results in Figure 9. For $\phi_1 = 0.94$ it is clear that, although intermolecular 1−1 contacts are slightly preferred near contact, in general, the segments of the two polymers are effectively randomly mixed. This rationalizes the result that the residual chemical potential changes on mixing for both components are effectively equal to zero in this range of composition. In contrast, at $\phi_1 = 0.06$, the segments of the two chains are nonrandomly mixed, with a definite bias towards preferring intermolecular 1−1 contacts. Following Guggenheim,[33] this nonrandom mixing effect should contribute to a negative partial molar entropy for component 1, a result that is qualitatively consistent with the positive chemical potential changes on mixing for this component in the $\phi_1 \rightarrow 0$ limit.

3.4. Discussion. We have shown that nonrandom packing effects appear to play a critical role in determining the chemical potential changes on mixing for the two different blend components. It is important to stress that, although many lattice models have incorporated the effects of nonrandom mixing[4,9,34] only a few recent models have incorporated these effects for off-lattice systems.[2,35] However, off-lattice and on-lattice theories and simulations all recognize and emphasize the role of nonrandom mixing ideas in obtaining a better understanding of polymer mixture thermodynamics.

We note that the different composition independent values of χ which appear to describe the chemical potential changes on mixing for the two components of the blends immediately implies that the single effective χ which describes the free energy of mixing would have a composition dependence.

$$\beta\Delta G_{\text{excess}} \equiv \phi_1\beta\Delta\mu_r^1 + \phi_2\beta\Delta\mu_r^2$$

$$= \phi_1\chi_1\phi_2^2 + \phi_2\chi_2\phi_1^2 \equiv \phi_1\phi_2[\chi_1\phi_2 + \chi_2\phi_1] \quad (27)$$

This linear composition dependence of the effective Flory interaction parameter has been observed in several blend systems, such as polystyrene/poly(vinylmethylether)[29] and poly(ethylene oxide)/poly(methyl methacrylate). While the linear composition dependence of χ values for these systems were derived from small angle neutron scattering, and could thus be affected by additional factors specific to the interpretation of scattering experiments,[14,29] nevertheless, we suggest that the nonrandom mixing observed here might serve to rationalize the thermodynamic behavior of this class of experimental situations.

It is also important to stress that although we have fit the chemical potential changes on mixing for each of the blend components in the attractive case with a composition-independent χ, this procedure violates thermodynamic consistency. To illustrate this point, we consider the Gibbs−Duhem relationship[28]

$$\left[\frac{\partial\mu_1}{\partial\ln\phi_1}\right]_{T,P} = \left[\frac{\partial\mu_2}{\partial\ln\phi_2}\right]_{T,P} \quad (28)$$

When applied to the attractive system this equality requires that

$$\chi_1 \equiv \chi_2$$

This, clearly, does not fit the data shown in Figure 4. Another means of reiterating this point is to derive the residual chemical potential changes on mixing from the Gibbs energy [eq 27], i.e.

$$\beta\Delta\mu_r^1 \equiv \left[\frac{\partial[(n_1 + n_2)\beta\Delta G_{\text{excess}}]}{\partial n_1}\right]_{T,P,n_2} \quad (29)$$

where n_i is the number of monomers of type i in the system of interest. If thermodynamic consistency is satisfied then $\beta\Delta\mu_r^1 = \chi_1\phi_2^2$ would be obtained from this procedure. Instead we obtain

$$\beta\Delta\mu_r^1 \equiv \chi''\phi_2^2 = \phi_2^2[\chi_1\phi_2 + \chi_2\phi_1 + \phi_1(\chi_2 - \chi_1)] \quad (30)$$

Similarly, for component 2, we expect $\beta\Delta\mu_r^2 = \chi_2\phi_1^2$, but we obtain

$$\beta\Delta\mu_r^2 \equiv \chi'''\phi_1^2 = \phi_1^2[\chi_1\phi_2 + \chi_2\phi_1 + \phi_2(\chi_1 - \chi_2)] \quad (31)$$

from the analog of eq 29 for component 2. This result conclusively demonstrates that the selection of different composition-independent values of χ to describe the chemical potential changes on mixing for the two blend components does not satisfy thermodynamic consistency. Further, the chemical potential changes on mixing that results from the free energy in eq 27 can only be described by an effective χ parameter which depends linearly on composition. In addition, the composition dependence of the χ parameters describing the two different components are not the same. We now consider component 1 in the limit $\phi_1 \rightarrow 0$. Clearly $\chi'' \equiv \chi_1$. In the limit $\phi_1 \rightarrow 1$, $\chi'' = 2\chi_2 - \chi_1$. Similarly, for $\phi_2 \rightarrow 0$, $\chi''' \equiv \chi_2$, while $\chi''' = 2\chi_2 - \chi_2$ when $\phi_2 \rightarrow 1$. It is clear that the two different composition independent values of χ, i.e., χ_1 and χ_2, derived from eq 13 and Figure

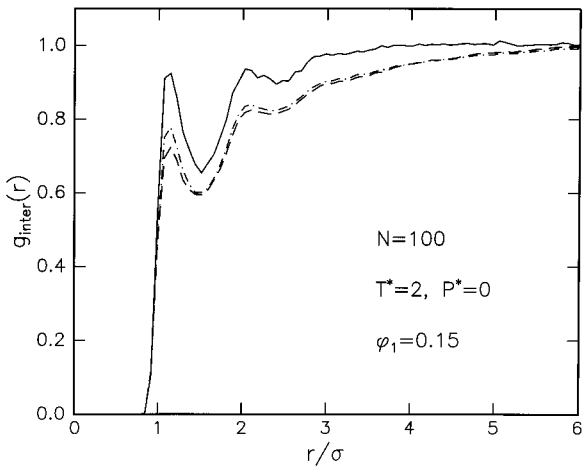

Figure 11. Plot of the three intermolecular radial distribution functions, $g_{ij,\text{inter}}(r)$, as a function of r for the nominally athermal blends comprised of chains of length $N = 100$ at $\phi_1 = 0.15$. Key: (—) 1−1 pairs; (− −) 2−2 pairs; and (− ·−) 1−2 pairs.

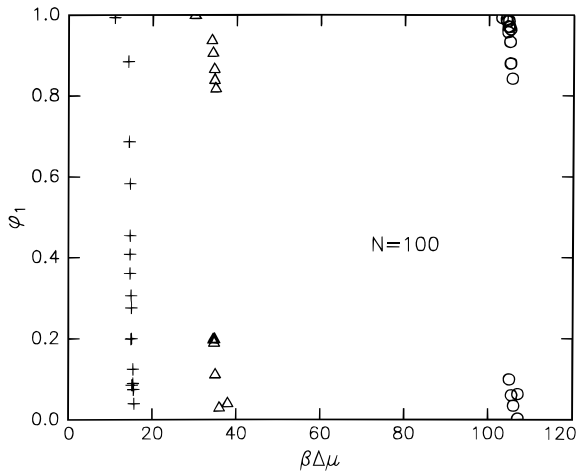

Figure 12. Plot of the average compositions in the simulation box, ϕ_1, as a function of the set value of the exchange chemical potential, $\beta\Delta\mu$, from the semigrand ensemble simulations. Key: (○) $T^* = 1$; (△) $T^* = 2$; (+) $T^* = 3$.

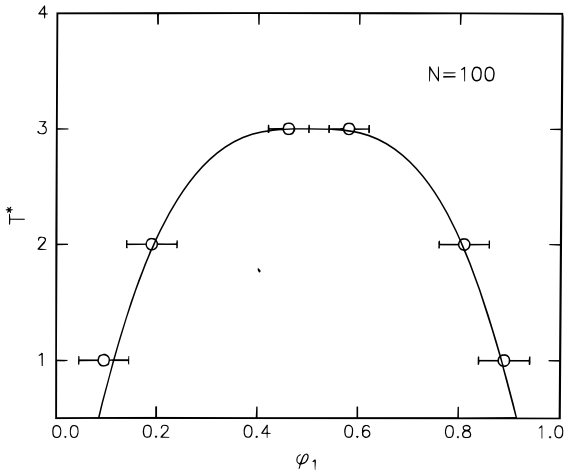

Figure 13. Computed phase diagrams plotted as T^* as a function of composition, ϕ_1, for the nominally athermal blend with $N = 100$. Points are simulation data, while the line is the scaling prediction from the Ising model.

4 are appropriate descriptors for the chemical potential changes on mixing in the respective infinite dilution limits. However, to satisfy thermodynamic consistency, the χ parameters in Figure 4 are not constants but must change with composition as derived above. Since our simulation data for chemical potential changes on mixing are only significantly different from zero close to the infinite dilution limit, it is clear that these data appear to be fit by composition-independent values of χ for each component. To summarize: thermodynamic consistency requires that the chemical potential changes on mixing must be described by χ values which are dependent on composition. However, for all practical purposes, it suffices to fit the simulation derived values of the chemical potential changes on mixing for each component with a composition independent χ, since $\beta\Delta\mu_r^i$ values are only sensitively different from zero in the infinite dilution limit where their dependence on composition is effectively parabolic.

4. Enumeration of Phase Diagrams for Nominally Athermal Systems

4.1. Results. We now consider the pair distribution functions for the nominally athermal mixtures comprised of chains of length $N = 100$, with $\phi_1 = 0.15$ in Figure 11. It is clear here that segments of type 1 are "clustering" together in a manner that is suggestive that this system might be on the verge of phase separation. We have attempted to locate the phase envelope by conducting simulations at a variety of compositions, dividing each simulation box into subboxes, and computing the static structure factor in each case. These calculations were inconclusive.

Subsequently, we have conducted simulations in the semigrand ensemble with the exchange chemical potential, $\Delta\mu$, as a parameter. Figure 12 shows results obtained at three different values of T^*. It is clear that the system composition shows discontinuous jumps in these plots, thus reiterating that we are observing a first-order phase transition, at least at the two lowest temperatures. Similar results, which are not shown for space reasons, were also observed for the system density. The situation at $T^* = 3$ is not so clear, and we conclude that this temperature is close to the critical value. As noted above we do not have an accurate means of determining the binodal compositions, and the phase diagrams that result from this approach (see Figure 13) are associated with significant error bars. The line drawn through the points in Figure 13 is a best fit to the Ising model prediction: $(\phi - \phi_c) \propto (T - T_c)^\beta$ where T_c is the critical temperature, ϕ_c is the critical composition, and $\beta = 1/3$. Since the uncertainties in the compositions of the two phases are relatively large we cannot determine the critical composition accurately. Therefore, we assigned $\phi_c = 0.5$ to reduce the number of fitting parameters. We have attempted to fit these coexistence curves to the mean-field exponent of $\beta = 1/2$ and obtained equally good fits. Consequently, these data could not be utilized to distinguish between the two models.

From these results, which have been reported briefly elsewhere,[22] we conclude that blends characterized by bare χ values of 0 in an incompressible, randomly mixed lattice sense need not be miscible at low temperatures and in fact can undergo liquid−liquid phase separation with an upper critical solution temperature. This fact cannot be captured by the standard Flory lattice model[3,32] (see eqs. 7 and 8). Since this model ignores the compressibility of the blend and assumes that chain segments mix randomly, the immiscibility of these systems reflects the failure of one or both of these approximations. The model of Sanchez[3] incorporates

the compressibility of the system but cannot reproduce the simulation results. Consequently, there appear to be two possible conclusions that can be drawn from these findings. First, it is possible that the theories of Sanchez and Flory incorporate enough analytical approximations that they are not accurate representations of the model systems. We cannot comment on this situation, but with this caveat, second, we suggest that compressibility effects by themselves cannot explain the findings. Additionally, the observed phase separation is probably not caused by excess volume changes on mixing since, in the single-phase region, the specific volumes of these nominally athermal blends are essentially arithmetic averages of the molar volumes of the pure components; i.e., the excess volume changes on mixing are equal to zero within simulation uncertainties. We also note that chain dimensions for the two species in each system do not change significantly on blending. Hence, conformational changes on mixing are probably not the cause for the observed demixing.

We therefore propose that the phase separation for these nearly symmetric systems arise primarily from the packing disparity inherent at the level of the pure components. Krishnamoorti and Graessley[13] have suggested that the phase behavior of hydrocarbon systems could be predicted by Flory−Huggins theory if χ is determined not by its bare definition as in eq 8 but by the relationship represented in eq 1. This approach has received further support from the recent work of Schweizer.[2] The rationale for utilizing this approach, which will discussed further below, is that the solubility parameter defined in eq 17 couples packing and energetic interactions when estimating the cohesive energy density of the system. Consequently, pure systems with stronger intermolecular interactions which pack better (see Figure 1) have larger solubility parameters than would be expected from random mixing models, such as Flory's, which ignore this packing effect. Consequently,[2,13] the χ parameter derived from this approach will provide a more reasonable estimate for the enthalpy change of mixing of this system. When utilized in conjunction with the Flory model, this approach should yield relatively accurate phase diagrams in these cases.

Following eq 1 yields $\chi \approx 0.05$ at $T^* = 2$ (Table 1), which suggests that chain mixtures longer than $N \approx 40$ would be immiscible at this temperature. This result is in reasonable agreement with our simulations. Note that the estimates presented here for χ and the critical chain length, which are our most reliable estimates, are slightly different from those reported earlier in ref 22. However, these differences are minor and reflect the inherent uncertainties in these calculations. Similar agreement between Flory theory and our simulations have been found at the two other temperatures considered, which suggests that the modification of Flory theory proposed by Krishnamoorti and Graessley[13] yields relatively accurate estimates of the phase diagram. These results emphasize that although the Lennard−Jones energetic parameters in these systems are matched so as to yield a bare $\chi = 0$; nevertheless, the most important disparity is caused by differences in intermolecular packing in the pure states. This aspect is anticipated by PRISM theory.[2]

In summary, we point to the fact that the differences in equation-of-state parameters for the two components in a polymer blend need not only cause the system to phase separate on heating.[7] Instead, we have demonstrated that small energetic asymmetries can cause polymer blends to phase separate with a well-defined UCST even when they are characterized by bare χ values of 0. We suggest that this behavior is a consequence of two polymeric phenomena. The first factor is the reduced entropy of mixing for polymers, as embodied in the 50 year old Flory−Huggins model.[32] The second contribution arises from the coupling between packing (or entropic) effects and attractive interactions which serves to destabilize these blends and cause phase separation. These findings prove that attaining miscibility in polymers is even more difficult than thought before and that strongly favorable interactions are generally necessary to achieve this goal.

4.2. Discussion. The important question to be resolved is that, although we have picked bare energetic interactions in a manner such that the nominal $\chi = 0$ as defined in eq 8, nevertheless, the enthalpy change on mixing is reasonably well described by a form represented by eq 1. To understand this issue we define the effective χ parameter

$$\chi \propto U_{12} - \frac{U_{11} + U_{22}}{2}$$

where U_{ij} is the net energy associated with an intermolecular $i-j$ interaction. It has, of course, been assumed in this analysis that the intramolecular interactions are unchanged when a chain is transferred from a pure melt to a blend, and hence we can focus on intermolecular interactions alone. U_{ij} is defined by the equation

$$U_{ij} = 2\pi\rho \int_0^\infty r^2 g_{\text{inter},ij}(r) u(r)\, dr \qquad (32)$$

In the Flory model $g_{\text{inter}}(r) = 1$, and hence χ defined in eq 8 is the relevant parameter for describing enthalpy changes on mixing. For the systems considered here, however, $g_{\text{inter}}(r) \neq 1$, and hence we need to reevaluate the enthalpy changes on mixing. Following Figure 11 we now assume that $g_{12}(r) = (g_{11}(r) + g_{22}(r))/2$. This assumption is not the most accurate representation of the data but is one which is sufficient to illustrate our point. One can now derive an equation for the effective χ parameter of the mixture

$$\chi \propto (\epsilon_{11} - \epsilon_{22})(I_{22} - I_{11}) \qquad (33)$$

where I_{jj} is defined in eq 21. From eq 33, several things are clear. First, a nonzero value of χ is driven almost exclusively by differences in packing behavior between the two components in the blend (or, in fact, in the pure state for this set of approximations). Such behavior cannot be captured by a theory that assumes random mixing of chain segments since $I_{11} = I_{22}$ in this case. Second, this packing disparity is driven by energetic differences as shown in Figure 1. In this specific case, both I_{11} and I_{22} are negative, with I_{11} having the larger absolute magnitude. Consequently, the χ parameter as defined in eq 33 is positive and favors demixing. It is therefore clear that the phase separation observed for these nominally athermal mixtures is driven by packing disparities which are caused by differences in energetic interactions at the level of the pure components. While eq 1 cannot be derived from a fundamental level, it is clear that this expression is approximately correct in this context since it reflects the importance of the coupling between energetic interactions and packing effects.

5. Conclusions

In this paper we have considered the thermodynamics and phase behavior of polymer blends where the energetic interactions of the pure components themselves are unequal. The consequence of this asymmetry manifests itself even at the level of the pure components, and the material with stronger bare interactions packs more efficiently. Other consequences of this packing disparity are that the density and the solubility parameters of the two pure materials are different. In the context of polymer mixtures, this packing asymmetry causes the chemical potential changes on mixing of the two components to be describable by linearly composition-dependent Flory interaction parameters, χ. This result is in qualitative accord with experimental results on several model polymer blends. Finally, this nonrandom mixing effect also causes polymer blends with nominal $\chi = 0$ in terms of the Flory lattice definition to phase separate. We show that this result is a consequence of the coupling between packing and energetic interactions which results in an unfavorable enthalpy change on mixing. We conclude by emphasizing the importance of packing effects in describing the thermodynamics of polymer systems, an issue which we have shown in this work to cause qualitative changes in the miscibility behavior of polymer systems.

Acknowledgment. Financial support from the National Science Foundation [CTS-9311915] is gratefully acknowledged. The author thanks Ken Schweizer and Jeff Weinhold for many useful discussions.

References and Notes

(1) Schweizer, K. S.; Curro, J. G. *J. Chem. Phys.* **1989**, *91*, 5059; *Phys. Rev. Lett.* **1988**, *60*, 809.
(2) Schweizer, K. S. *Macromolecules* **1993**, *26*, 6050. Schweizer, K. S.; Singh, C. *Macromolecules* **1995**, *28*, 2063. Singh, C.; Schweizer, K. S. *Macromolecules* **1995**, *28*, 8692.
(3) Lacombe, R. H.; Sanchez, I. C. *J. Phys. Chem.* **1976**, *80*, 2568.
(4) Freed, K. F. *J. Chem. Phys.* **1988**, *88*, 5871.
(5) Sariban, A.; Binder, K. *J. Chem. Phys.* **1987**, *86*, 5859; *Macromolecules* **1988**, *21*, 711; *Makromol. Chem.* **1988**, *189*, 2357; *Colloid Polym. Sci.* **1989**, *267*, 469.
(6) Deutsch, H.-P.; Binder, K. *Europhys. Lett.* **1992**, *17*, 697. *Macromolecules* **1992**, *25*, 6214.
(7) Sanchez, I. C. Polymer Compatibility and Incompatibility. *MMI Press Symp. Ser.* **1976**, *80*, 2568.
(8) Sanchez, I. C. *Annu. Rev. Mater. Sci.* **1983**, *13*, 387.
(9) Panayiotou, C.; Vera, J. H. *Polymer* **1982**, *14*, 681.
(10) Flory, P. J. *J. Chem. Phys.* **1941**, *9*, 660.
(11) Huggins M. L. *J. Phys. Chem.* **1942**, *46*, 151.
(12) Bates F. S.; Muthukumar, M.; Wignall, G. D.; Fetters, L. J. *J. Chem. Phys.* **1988**, *89*, 535.
(13) Krishnamoorti, R. Ph.D. Thesis, Princeton University, 1994.
(14) Kumar, S. K. *Macromolecules* **1994**, *27*, 260.
(15) Kumar, S. K.; Szleifer, I.; Panagiotopoulos, A. Z. *Phys. Rev. Lett.* **1991**, *66*, 2935.
(16) Kumar, S. K. *J. Chem. Phys.* **1992**, *96*, 1492.
(17) Szleifer, I.; Panagiotopoulos, A. Z. *J. Chem. Phys.* **1992**, *97*, 6666.
(18) Kumar, S. K. *Fluid Phase Equil.* **1993**, *83*, 333.
(19) Weinhold, J. D.; Kumar, S. K.; Singh, C.; Schweizer, K. S. *J. Chem. Phys.* **1995**, *103*, 5814.
(20) Sheng, Y.-J.; Panagiotopoulos, A. Z.; Kumar, S. K. *J. Chem. Phys.* **1995**, *103*, 10315.
(21) Sanchez, I. C. Preprint.
(22) Kumar, S. K.; Weinhold, J. D. *Phys. Rev. Lett.* **1996**, *77*, 1512.
(23) Kofke, D. A.; Glandt, E. D. *Mol. Phys.* **1988**, *64*, 1105.
(24) Hildebrand, J. H.; Scott, R. L. *The Solubility of Non-Electrolytes*, 3rd ed.; Dover: New York, 1964.
(25) Allen, M. P.; Tildesley, M. P. *Computer Simulations of Liquids*; Oxford University Press: New York, 1987.
(26) Panagiotopoulos, A. Z. *Mol. Simul.* **1992**, *9*, 1.
(27) Escobedo, F.; dePablo, J. J. Preprint.
(28) Prausnitz, J. M.; Lichtenthaler, R. N.; de Azevedo, E. G. *Molecular Thermodynamics of Fluid-Phase Equilibria*; Princeton Hall: Englewood Cliffs, NJ, 1986.
(29) Taylor, J. K.; Debenedetti, P. G.; Graessley, W. W.; Kumar, S. K. *Macromolecules* **1996**, *29*, 764.
(30) Debenedetti, P. G.; Kumar, S. K. *AIChE J.* **1986**, *32*, 1253.
(31) Briber, R. M. *J. Chem. Phys.*, **1994**, *101*, 2592.
(32) Flory, P. J. *Principles of Polymer Chemistry*; Cornell University Press: Ithaca, NY, 1953.
(33) Guggenheim, E. A. *Mixtures*; Clarendon Press: 1954.
(34) Freed, K. F.; Dudowicz, J. *Theor. Chim. Acta* **1992**, *82*, 357.
(35) Taylor, M. P.; Lipson, J. E. G. *J. Chem. Phys.* **1995**, *102*, 6272.

MA961348A